Proceedings of the 7th World Congress on Momentum, Heat and Mass Transfer (MHMT'22)
~~Lisbon, Portugal~~ Virtual Conference – April 07 – 09, 2022
Paper No. ENFHT 194
DOI: 10.11159/enfht22.194

Experiment and Molecular Dynamics Analysis on Enhanced Evaporation of Silver Nanofluids under Light Irradiation

Chang Zhao, Wei An*, Yifan Zhang, Qingchun Dong, Naiping Gao
College of Mechanical Engineering, Tongji University, Shanghai, P.R. China

Abstract Recently, some studies have shown that the vaporization of plasmonic nanofluids (PNFs) is observed to be more intensive than that of pure water during the light-induced heating process, but the mechanism remains controversial. In this work, we conduct several comparative experiments and molecular dynamics (MD) simulations to investigate the evaporation process of PNFs under the illumination of different monochromatic incident lights, especially focusing on the plasma-mediated evaporation mechanism. Based on the experimental results of silver and graphite nanofluids, it is found that the evaporation process of silver nanofluids can be heavily promoted under the combined effect of the enhanced electric field induced by the localized surface plasmon resonance (LSPR) and the thermal diffusion. Combined with the electromagnetic theory, a modified MD simulation is developed to analyze the effect of the induced electric field on the evaporation process of silver nanofluids. The results indicate that nanoparticles with the LSPR effect are not only 'heat sources' which transfer the thermal energy to the surrounding media, but also can produce the enhanced electric field to directly impact the motion of water molecules. The effect of localized electric field on the evaporation of PNFs cannot be neglected. The results also reveal that the light-induced evaporation process of PNFs is quite different from the conventional thermo-mediated evaporation process in carbon-based nanofluids. This work can offer some new insights for a comprehensive understanding of the evaporation process of PNFs, which is of fundamental interest to many emerging applications.

***Keywords*:** silver nanofluids, evaporation, surface plasmon resonance, enhanced electric field

1. Introduction

Fluid evaporation is a fundamental process in daily life, and evaporation manipulation has been used in some industries such as energy, electricity, petrochemical, aerospace, etc. [1,2]. Due to the localized surface plasmon resonance (LSPR) effect [3], some metal and semiconductor nanoparticles can tune their optical properties flexibly. Therefore, the addition of these nanoparticles into pure liquids can form nanofluids, which have been of great interest for several emerging applications, i.e., solar energy usage [4,5], optofluidic control [6,7], and biomedicine [8,9]. Among these applications, the role of the evaporation process cannot be neglected. For instance, after adding plasmonic nanoparticles (PNPs), the evaporation efficiency of liquids can be dramatically raised under the illumination of solar energy [4]. In the application of optofluidic control, the vaporized gas becomes a crucial factor to drive and guide the motion of nanofluids [6]. Under laser irradiation, nanobubbles of various sizes can be utilized in drug delivery and the destruction of cancer cells [8]. Hence, it is necessary to perform an in-depth study on the light-induced evaporation mechanism of plasmonic nanofluids (PNFs) to provide some valuable theoretical guidance for these emerging technologies.

To date, there are some controversies about the pathways of energy conversion during the evaporation process, and there is still a lack of comprehensive research on the evaporation mechanism of PNFs. In the conventional thermo-mediated evaporation process, the energy of incident irradiation is absorbed by the free electrons on the surface of PNPs and transferred to the metal lattice through electron-phonon interactions, which leads to an increase in the temperature of PNPs. Therefore, PNPs are treated as localized heat sources that diffuse the photo-induced heat to the surrounding fluids through conduction and convection [10,11]. As the heat accumulates in the PNPs, the spinodal temperature of water can be exceeded, which results in the formation of nanobubbles [12-14]. However, other investigations have revealed a totally different mechanism from thermo-mediated evaporation. Lachaine et al. proposed that nanobubbles can be induced directly by plasma instead of thermal energy under the irradiation of a pulsed laser [15]. Neumann et al. found that nearly 80% of the absorbed energy is used for steam generation, and only 20% is used for heating fluids under the illumination of solar energy [16]. In fact, when the LSPR effect is excited, the oscillation of free electrons, known as surface plasma, can produce a localized electric field with very high intensity on the surface of PNPs [17,18]. Therefore, during the light-induced heating PNFs, the absorbed energy is not only transformed into thermal energy, but also an enhanced electric field

on the surface of particles. However, previous studies always associated the plasma-mediated evaporation with short-pulsed lasers, but rarely mentioned in the case under the continuous incident light illumination, and few reports have focused on the LSPR-induced localized electric field.

Recently, some studies have demonstrated that the movements of water molecules can be affected in the presence of a localized electric field. Using the molecular dynamics (MD) simulation, Okuno et al. found that for pure water, the motion of water molecules and the structure of hydrogen bonds can be changed under a uniform electric field [19]. For nanofluids, the evaporation process can be accelerated under a uniform electric field [20,21]. When nanofluids were subjected to an alternating electric field with the square wave, Zhang et al. found that the evaporation process can also be enhanced [22]. Unfortunately, none of these above works considered the LSPR effect, and although monochromatic incident lights at various wavelengths were used to heat nanofluids in some experiments [23,24], the effect of the induced enhanced electric field was still not mentioned yet.

In this work, the evaporation process of silver and graphite nanofluids under the illumination of the continuous monochromatic lights was analyzed by several comparative experiments. Moreover, a model based on the MD simulation and electromagnetic theory was developed to reveal the effect of the localized electric field on the evaporation of PNFs.

2. Experimental Design

To study the effect of the LSPR-induced electric field on the evaporation process, silver nanofluids were irradiated with monochromatic incident lights. Besides, as a type of carbon-based material, graphite nanofluids were heated as a comparison test. As shown in Fig. 1(a) to (b), the morphology of silver nanoparticles (Shanghai So-Fe biomedicine Co., Ltd., China) is found as an ellipsoid, while that of graphite nanoparticles (Shanghai ACMEC biomedical Co., Ltd., China.) is a sphere approximately.

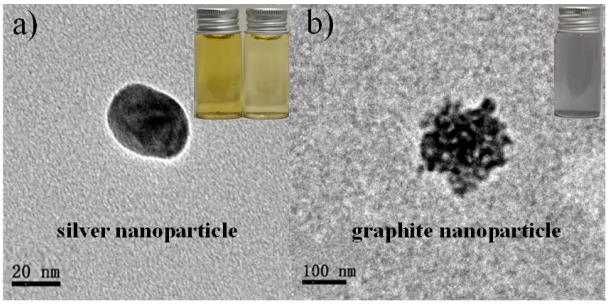

Fig. 1: TEM image of (a) silver nanoparticles; (b) graphite nanoparticles

The transmittance of different nanofluids was measured by a spectrometer (PG2000, Ideaoptics). As shown in Fig. 2(a), the LSPR effect of silver nanofluids can be excited under the irradiation at 460 nm, while it cannot occur under the illumination at 945 nm; and there is no LSPR effect for graphite nanofluids at visible-light waveband.

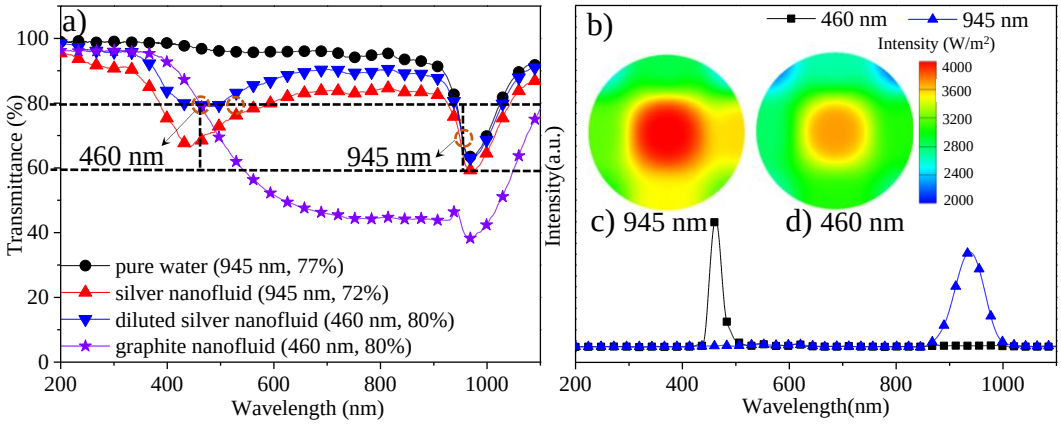

Fig. 2: Properties of nanofluids and incident light sources: (a) transmittance of nanofluids; (b) the spectra of incident lights; (c)-(d) the power distribution of incident light sources

Due to different light absorption capacities, the absorbed energy for these nanofluids was also different under the illumination of monochromatic light with various wavelengths. In order to eliminate the influence of the difference in absorption capacity on the experiment, it was necessary to adjust the transmittance of these nanofluids to the same value as much as possible in each comparative test. Therefore, as shown in Fig. 2(a), the transmittance of silver nanofluids at 945 nm is tuned to 72%, which is very close to that of pure water. Similarly, the transmittance of diluted silver nanofluids at 460 nm is tuned to 80%, which is the same as that of graphite nanofluids at 460 nm. After adjusting the transmittance, the nanofluid concentration was measured by an inductively coupled plasma optical emission spectrometry (ICP-OES, Thermo-Fisher Corp.), as listed in Table 1.

Table 1. Concentrations of different nanofluids

Nanofluids	Concentration (μg/mL)
diluted silver nanofluids	3.0
silver nanofluids	8.8
graphite nanofluids	77.0

As depicted in Fig. 2(b), two monochromatic LED light sources were used to heat these nanofluids. The emission wavelength of the light source was 460 nm, which corresponded to the resonance peak of silver nanofluids. Moreover, the LED with an emission wavelength at 945 nm was also used as the comparative light source, because pure water has an absorption effect at this wavelength, but silver nanofluids cannot produce the LSPR effect at 945 nm. After adjusting the transmittance of different PNFs, the incident power of each light source also should be tuned to an identical value to reduce the discrepancy in energy absorption. However, in practice, it was rather difficult to adjust the power of LED light sources at different wavelengths to the same value because the light intensity distribution of different LED sources was non-uniform as shown in Fig. 2(c) to (d). To emphasize the LSPR effect on the evaporation process, it was reasonable to make the energy absorbed by the silver nanofluids under the illumination at 460 nm slightly less than that absorbed at 945 nm, as shown in Fig. 2(a).

As shown in Fig. 3, an experimental system was built to compare the evaporation process of different nanofluids. In the test, 23 g nanofluids were placed in a petri dish and form a liquid film with a thickness of approximately 5 mm. A balance (Sartorius, BSA124S) was used to measure the fluid mass in the experiment. To measure the nanofluid temperature, an infrared thermometer (MLX90614) with an accuracy of 0.1°C was aimed at the surface of the petri dish to monitor the surface temperature of the fluid, and a K-type thermocouple with a precision of 0.1 °C was pasted on the bottom of the petri dish without touching the underside to measure the inner temperature of the fluid.

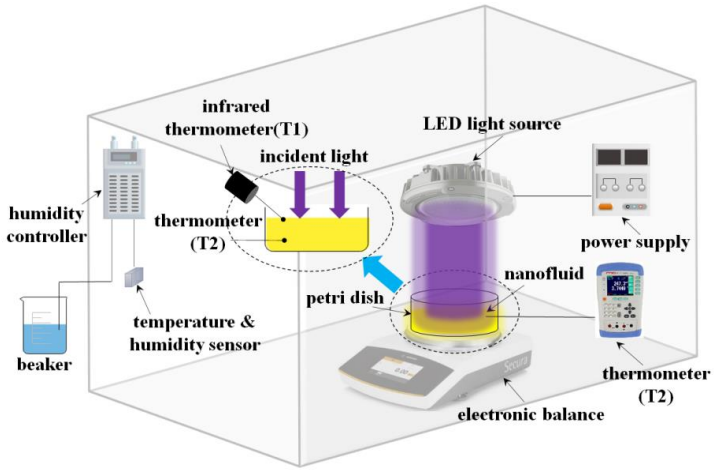

Fig. 3: Sketch of the evaporation experiment system

During the experiments, to ensure that the evaporation environment was as similar as possible, all experiments were performed in a sealed chamber made of polymethyl methacrylate with a small dehumidifier fixed inside to maintain the testing environment at a temperature of 32-34 °C and a humidity of 54%-58%, respectively. The evaporation experiments were performed in three groups, and each group was repeated three times. In each experiment, the fluids were heated for 40 minutes, and the data were recorded every minute.

3. Experimental Results And Discussion

3.1 Silver Nanofluids With and Without the LSPR Effect

The evaporation experiments of silver nanofluids were performed under light heating at 460 nm and 945 nm, respectively. As shown in Fig. 4(a), the evaporation mass of silver nanofluids can reach 1076.2 mg under the illumination at 945 nm, and that of pure water is 1109.6 mg. However, under the illuminated at 460 nm, the evaporation mass of diluted silver nanofluids reaches 1497.6 mg, which is 421.4 and 388.0 mg higher than that of silver nanofluids and pure water illuminated at 945nm, respectively. It is worth noting that, as shown in Fig. 2(a), the transmittance of pure water and silver nanofluids at 945 nm is lower than that of diluted silver nanofluids illuminated at 460 nm. This indicates that the evaporation of diluted silver nanofluids is more intensive under the irradiation at 460 nm than that of pure water and silver nanofluids irradiated at 945nm, though the two latter absorb more light energy.

Moreover, from Fig. 4(b), it can be found that the internal temperature rise (T2) of diluted silver nanofluids is far higher than that of pure water and silver nanofluids. In addition, the internal temperature rise (T2) of diluted silver nanofluids is always higher than its surface temperature rise (T1). Such a temperature distribution is not surprising, and similar phenomena have been discussed in some works by Jang et al. and An et al. [25,26]. The work by Yun et al. indicated the radiative transfer in the semitransparent media is the crucial factor that leads to such peculiar temperature distribution [27]. Therefore, enhanced evaporation can be observed owing to the LSPR effect, which is reflected in the increase in the evaporation mass and the rise of the internal temperature.

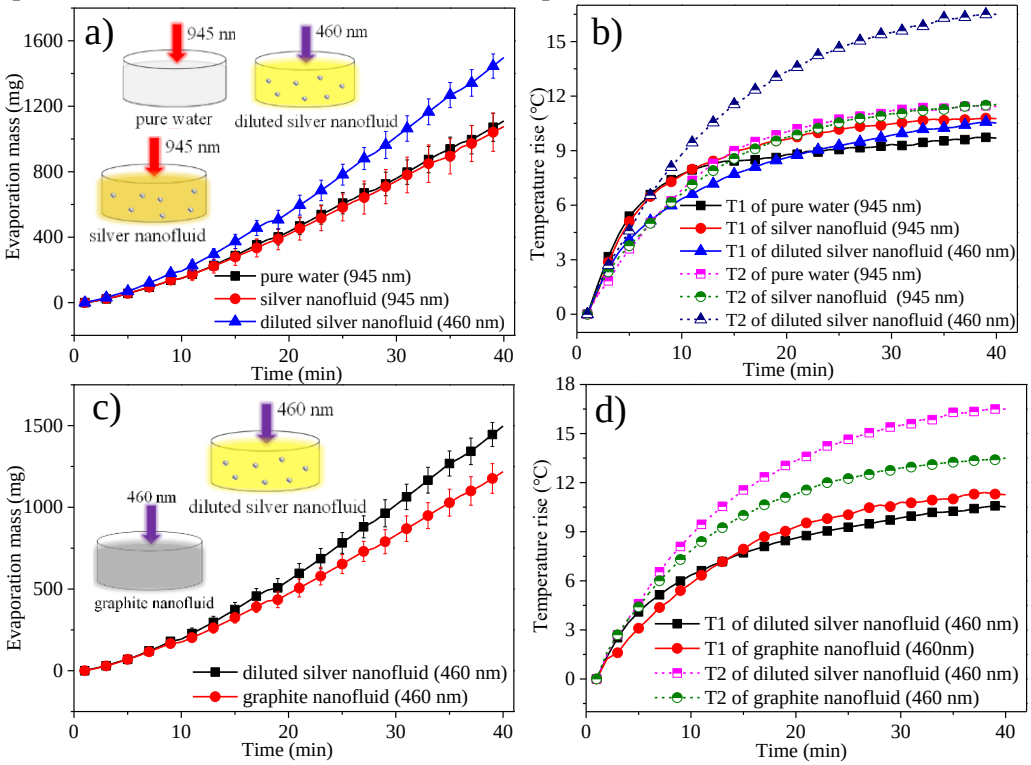

Fig. 4: Experimental results of evaporation mass and temperature rise: (a)-(b) silver nanofluids and pure water under the illumination at 460 nm and 945 nm; (c)-(d) silver and graphite nanofluids under the illumination at 460 nm

3.2 Silver and Graphite Nanofluids under the Same Illumination Condition

Fig. 4(c) demonstrates that the evaporation mass of graphite nanofluids can reach 1218.2 mg, which is also 279.4 mg less than that of diluted silver nanofluids under the same heating condition at 460 nm. Moreover, as shown in Fig. 4(d), the internal temperature of silver nanofluid is higher than that of graphite nanofluid, while their surface temperature has an opposite trend. It also indicates that the evaporation process of diluted silver nanofluid is more intensive than that of graphite nanofluids when they are under the same heating conditions with the same transmittance at 460 nm.

In summary, under the illumination at 460 nm, the diluted silver nanofluids show intensive evaporation and higher internal temperature than that of pure water and graphite nanofluids. Therefore, we can obtain the following conclusions:

1) As depicted in Fig. 4(a), even if two identical nanofluids are under the light-induced heating process, the obvious different evaporation process can be found due to different illumination conditions. When the frequency of incident light is close to the plasmon resonance wavelength of the nanofluids, the evaporation process can be obviously accelerated by the LSPR effect of nanoparticles.

2) As shown in Fig. 4(c), even at the same light absorption, the evaporation of silver nanofluid is more intensive than that of the graphite nanofluid. Thus, the LSPR-enhanced evaporation is more intensive than the only thermo-mediated evaporation.

From the above experimental results, it is found that the LSPR effect can significantly influence the evaporation process of PNFs. However, only the above experiments are not enough to clearly explain the mechanism difference between the thermo-mediated and the plasma-mediated evaporation. To reveal the reasons behind these phenomena, we continue to carry out a MD simulation in the following part.

4. MD simulation for LSPR-enhanced evaporation

4.1 Localized Electric Field on the Surface of Silver Nanoparticles

Under the plasma resonance effect, a localized electric field can be produced on the silver nanoparticle surface. Therefore, a near-field radiation model based on the Finite Difference Time Domain (FDTD) method was developed to calculate the distribution of the localized electric field. As shown in Fig. 5, the intensity of the electric field on the surface of silver nanoparticles is very high, while no obvious LSPR is observed for graphite nanoparticles at 200-800 nm. It demonstrates that the water molecules near silver nanoparticles can suffer a strong electric field force. Based on the electromagnetic theory[28], the field enhancement coefficient of silver nanoparticles is set as 300, and the intensity of the localized electric field for silver nanoparticles is determined as 1.7×10^{-4} V/Å with the period of 2.0 fs in the following MD simulation.

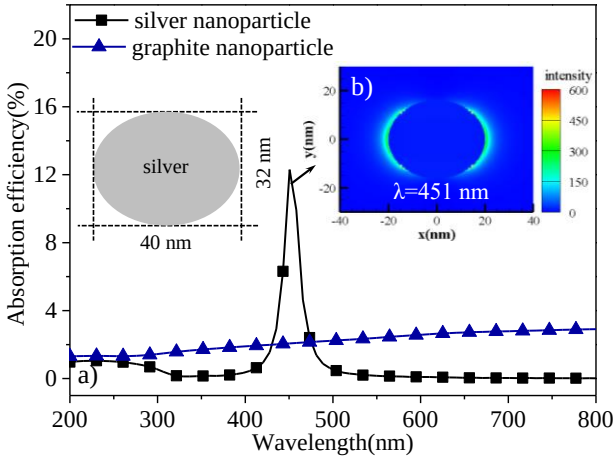

Fig. 5. FDTD simulation results: (a) absorption spectra of silver nanoparticles and graphite nanoparticles; (b) the intensity distribution of the localized electric field on the surface of silver nanoparticles

4.2 Evaporation Process Simulation

To investigate the effect of the LSPR-enhanced evaporation process, a model based on the MD simulation was developed. As illustrated in Fig. 6, a simulation box with the size of 5 nm × 5 nm × 20 nm was built on the surface of silver nanoparticles. Silver atoms were arranged at the bottom of the simulation box with a thickness of 0.8 nm. Water molecules with the number of 3887 were placed on the surface of silver atoms to form a liquid film with a thickness of 8 nm. The bottom layer of silver atoms was fixed to prevent deformation, and the other layers were modeled as the thermostat. The water molecules were fixed by the shake algorithm during the simulation [29,30]. Periodic boundaries were imposed on the x-direction and y-direction, and a fixed boundary was set on the z-direction. A vapor region with a thickness of 2.0 nm was defined at the top of the simulation box, and water molecules were eliminated from the simulation box when they arrived at this region. This model included the thermo-induced and plasma-induced effects on the evaporation process. Thus, the temperatures of silver atoms and water film were first maintained at 300 K for 100 ps using a Nose-Hoover thermostat

[31].

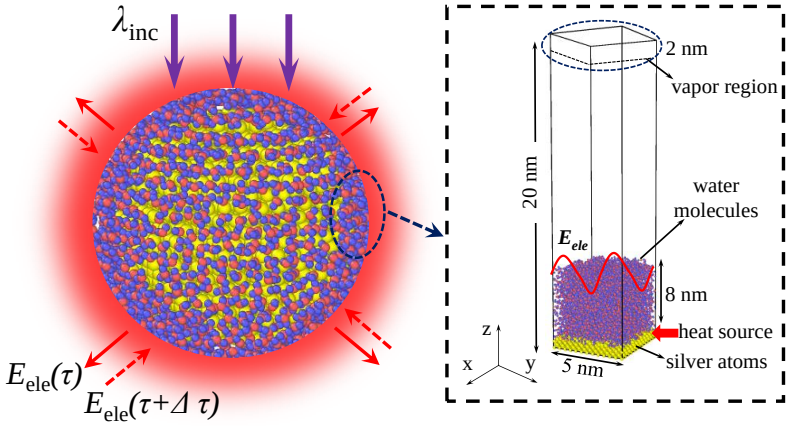

Fig. 6. The model of MD simulation for the LSPR-enhanced evaporation process

After reaching the equilibrium state, the silver atoms and water film were maintained at different temperatures according to the simulation cases, as shown in Fig. 7. If the LSPR effect is not considered, the temperature of the silver atoms and the water film was maintained at 319 K, which was the temperature of the silver nanofluids under the irradiation at 945 nm for 40 minutes. When the LSPR effect is considered, the temperature of the silver atoms was maintained at 465 K according to the work by Fang et al. [12]. Based on the above experimental results, the temperatures of the water film on the surface of silver atoms were set to 324 K. When the temperature of the silver atoms reached the desired value, they were treated as heat sources to transfer thermal energy, and an additional alternating electric field was applied on the water film in the x-direction. The intensity and period of the additional alternating electric field were set according to the above results by the near-field radiation model. All simulations were conducted using the Large-Scale Atomic/Molecular Massively Parallel Simulator (LAMMPS) software package.

4.3 Results analysis of MD simulation

The snapshots of simulation results were displayed in Fig. 7 to analyze the evolution of the evaporation process. From Fig. 7(a), it can be found that water molecules are tightly constrained on the silver atom surface when the LSPR effect is not considered. The restriction of the motion of water molecules leads to a slightly smaller evaporation mass of silver nanofluids than that of pure water under the illumination at 945 nm, as the experimental results shown in Fig. 4(a). When the LSPR effect is excited, Fig. 7(b) displays that the water film thickness is gradually decreased due to the combined effect of thermal diffusion and enhanced electric field. It is also consistent with the experimental results that the evaporation mass of silver nanofluids under the illumination at 460 nm is higher than that irradiated at 945 nm, as shown in Fig. 4(a).

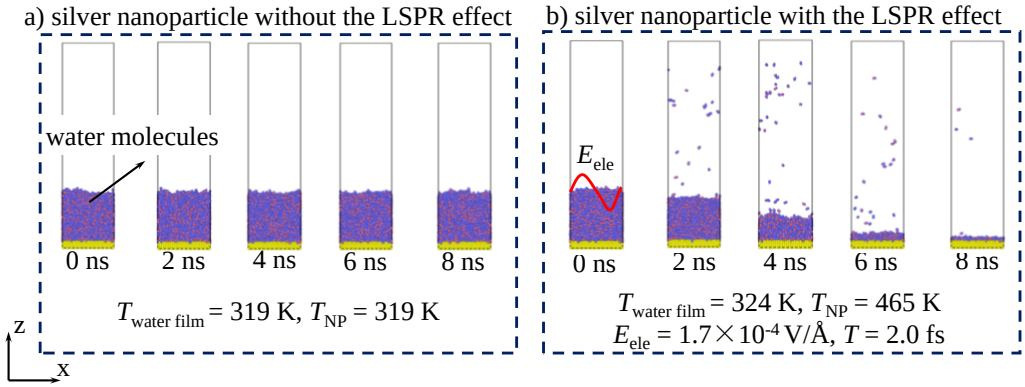

Fig. 7. Transient snapshots for the evaporation process of water film: (a) on silver atom surface without the LSPR effect; (b) on silver atom surface with the LSPR effect

To compare the evaporation velocity of different simulation cases, we calculated the number of evaporated water molecules in a period. As listed in Table 2, the evaporation velocity of the water film on the surface of silver atoms is very

slow when the LSPR effect is not excited. While the evaporation velocity dramatically increases to 1780×10^{-26} kg/ns when the LSPR effect is considered. Moreover, the evaporation velocity of the silver nanofluids increases by 20% under the LSPR including thermal and plasma combined effect than the case of only considering the thermal effect. The above results indicate that the effect of the enhanced electric field cannot be neglected in the light-induced evaporation process of PNFs.

Table 2. Evaporation velocity of the water film on silver atom surface for different cases

Simulation cases		Evaporation velocity (10^{-26} kg/ns)
silver	without the LSPR effect	12
	only thermal effect	1483
	thermal and plasma combined effect	1780

5. Conclusion

In the present work, we revealed that the important role of the enhanced electric field in the light-induced evaporation process of silver nanofluids through experiments and MD simulations. In the experiments, the evaporation process of silver and graphite nanofluids was comparatively tested under the illumination of monochromatic light sources at different wavelengths. The experimental results show that the LSPR effect has a strong accelerating effect on the evaporation process of silver nanofluids. Meanwhile, we developed a MD model combined with electromagnetic theory to investigate the LSPR-enhanced evaporation process. It can be found that when the LSPR effect is excited, the evaporation process of silver nanofluids can be significantly enhanced by the combined effect of the thermal diffusion and the enhanced electric field on the nanoparticles. Unlike the thermal diffusion effect, the enhanced electric field on the nanoparticle surface can affect water molecules more rapidly and directly, causing them to oscillate violently and periodically, thus accelerating the evaporation process. It is totally different from the conventional thermo-mediated mechanism in fluid evaporation.

In conclusion, there are two different evaporation mechanisms during the evaporation process of PNFs under continuous light irradiation, one is the generally accepted thermo-mediated evaporation mechanism, and the other is the electric-field-mediated evaporation mechanism. The LSPR-enhanced electric field has a significant effect on the motion of surrounding water molecules, especially during the initial evaporation period with a relatively low particle temperature. Notably, the surface temperature of the nanoparticles is not accurately measured in the present work, and the evaporation process of PNFs with different materials such as gold nanofluids is also not considered. For these issues, further investigations will be performed in our future work.

Acknowledgments

This work was supported by the Natural Science Foundation of Shanghai (No. 20ZR1459600) and the Fundamental Research Funds for the Central Universities of China, all of which are gratefully acknowledged.

References

[1] O. Mahian, E. Bellos, C. N. Markides, R. A. Taylor, A. Alagumalai, L. Yang, C. Qin, B. J. Lee, G. Ahmadi, M. R. Safaei, and S. Wongwises, "Recent advances in using nanofluids in renewable energy systems and the environmental implications of their uptake," *Nano Energy,* vol. 86, pp. 106069, 2021.

[2] Z. Liu, F. Fontana, A. Python, J. T. Hirvonen, and H. A. Santos, "Microfluidics for Production of Particles: Mechanism, Methodology, and Applications," *Small,* vol. 16, pp. 1904673, 2019.

[3] X. Fan, W. Zheng and D. J. Singh, "Light scattering and surface plasmons on small spherical particles," *Light: Science & Applications,* vol. 3, pp. e179, 2014.

[4] R. A. Taylor, T. Otanicar and G. Rosengarten, "Nanofluid-based optical filter optimization for PV/T systems," *Light: Science & Applications,* vol. 1, pp. e34, 2012.

[5] O. Mahian, A. Kianifar, S. A. Kalogirou, I. Pop, and S. Wongwises, "A review of the applications of nanofluids in solar

energy," *International Journal of Heat and Mass Transfer,* vol. 57, pp. 582-594, 2013.
[6] J. Kim, L. P. Lee, G. L. Liu, and Y. Lu, "Optofluidic control using photothermal nanoparticles," *Nature materials,* vol. 5, pp. 27-32, 2006.
[7] Y. Li, Y. Ren, H. Qi, and L. Ruan, "Manipulation of Microscale Fluid Using Laser-Irradiated Nanoparticle Arrays," *Plasmonics,* vol. 14, pp. 1555-1563, 2019.
[8] A. Shakeri-Zadeh, H. Zareyi, R. Sheervalilou, S. Laurent, H. Ghaznavi, and H. Samadian, "Gold nanoparticle-mediated bubbles in cancer nanotechnology," *Journal of Controlled Release,* vol. 330, pp. 49-60, 2021.
[9] Y. Bayazitoglu, S. Kheradmand and T. K. Tullius, "An overview of nanoparticle assisted laser therapy," *International Journal of Heat and Mass Transfer,* vol. 67, pp. 469-486, 2013.
[10] X. Chen, Y. Chen, M. Yan, and M. Qiu, "Nanosecond Photothermal Effects in Plasmonic Nanostructures," *ACS Nano,* vol. 6, pp. 2550-2557, 2012.
[11] R. A. Ganeev, A. I. Ryasnyansky, S. R. Kamalov, M. K. Kodirov, and T. Usmanov, "Nonlinear susceptibilities, absorption coefficients and refractive indices of colloidal metals," *Journal of physics. D, Applied physics,* vol. 34, pp. 1602-1611, 2001.
[12] Z. Fang, Y. Zhen, O. Neumann, A. Polman, F. J. García De Abajo, P. Nordlander, and N. J. Halas, "Evolution of Light-Induced Vapor Generation at a Liquid-Immersed Metallic Nanoparticle," *Nano Letters,* vol. 13, pp. 1736-1742, 2013.
[13] Y. Wang, M. E. Zaytsev, H. L. The, J. C. T. Eijkel, H. J. W. Zandvliet, X. Zhang, and D. Lohse, "Vapor and Gas-Bubble Growth Dynamics around Laser-Irradiated, Water-Immersed Plasmonic Nanoparticles," *ACS Nano,* vol. 11, pp. 2045-2051, 2017.
[14] Y. Tabayashi, S. Sakaki, N. Koshizaki, Y. Yamauchi, and Y. Ishikawa, "Behavior of Thermally Induced Nanobubbles during Instantaneous Particle Heating by Pulsed Laser Melting in Liquid," *Langmuir,* vol. 37, pp. 7167-7175, 2021.
[15] R. Lachaine, É. Boulais and M. Meunier, "From Thermo- to Plasma-Mediated Ultrafast Laser-Induced Plasmonic Nanobubbles," *ACS Photonics,* vol. 1, pp. 331-336, 2014-04-16 2014.
[16] O. Neumann, A. S. Urban, J. Day, S. Lal, P. Nordlander, and N. J. Halas, "Solar Vapor Generation Enabled by Nanoparticles," *ACS Nano,* vol. 7, pp. 42-49, 2012.
[17] J. Duan, X. Li, L. Yao, S. Pan, and M. Chen, "Local field enhancement of pair arrays of silver nanospheres," *Optics Communications,* vol. 282, pp. 4005-4008, 2009.
[18] D. Li, X. Sun, Y. Jia, M. I. Stockman, H. P. Paudel, H. Song, H. Jiang, and Z. Li, "Direct observation of localized surface plasmon field enhancement by Kelvin probe force microscopy," *Light: Science & Applications,* vol. 6, pp. e17038, 2017.
[19] Y. Okuno, M. Minagawa, H. Matsumoto, and A. Tanioka, "Simulation study on the influence of an electric field on water evaporation," *Journal of Molecular Structure: THEOCHEM,* vol. 904, pp. 83-90, 2009.
[20] B. Wang, X. Wang, Y. Duan, and M. Chen, "Molecular dynamics simulation on evaporation of water and aqueous droplets in the presence of electric field," *International Journal of Heat and Mass Transfer,* vol. 73, pp. 533-541, 2014.
[21] B. Wang, H. Zhang, Z. Xu, X. Wang, Q. Zhao, and W. Yan, "Acceleration of aqueous nano-film evaporation by applying parallel electric field: A molecular dynamics simulation," *International Journal of Heat and Mass Transfer,* vol. 138, pp. 68-74, 2019.
[22] H. Zhang, B. Wang, Z. Xu, X. Li, and W. Yan, "Molecular dynamics simulation on evaporation enhancement of water and aqueous nano-films by the application of alternating electric field," *International Journal of Heat and Mass Transfer,* vol. 145, pp. 118735, 2019.
[23] H. Chen, L. Shao, T. Ming, Z. Sun, C. Zhao, B. Yang, and J. Wang, "Understanding the Photothermal Conversion Efficiency of Gold Nanocrystals," *Small,* vol. 6, pp. 2272-2280, 2010.
[24] M. Chen, Y. He, Q. Ye, X. Wang, and Y. Hu, "Shape-dependent solar thermal conversion properties of plasmonic Au nanoparticles under different light filter conditions," *Solar Energy,* vol. 182, pp. 340-347, 2019.
[25] B. Jang, Y. S. Kim and Y. Choi, "Effects of Gold Nanorod Concentration on the Depth-Related Temperature Increase During Hyperthermic Ablation," *Small,* vol. 7, pp. 265-270, 2011.
[26] W. An, Q. Zhu, T. Zhu, and N. Gao, "Radiative properties of gold nanorod solutions and its temperature distribution under laser irradiation: Experimental investigation," *Experimental Thermal and Fluid Science,* vol. 44, pp. 409-418, 2013.
[27] Q. Yun, H. Tan, "Numerical analysis of temperature field in materials during infrared heating," *Journal of Infrared Miller Waves*, vol. 10, pp. 147-155, 1991.
[28] C. Zhao, W. An and N. Gao, "Light-induced latent heat reduction of silver nanofluids: A molecular dynamics simulation," *International Journal of Heat and Mass Transfer,* vol. 162, pp. 120343, 2020.
[29] H.J.C. Berendsen, J.R. Grigera, T. P. Straatsma, "The missing term in effective pair potential," *J. Phys. Chem*. vol. 91, pp. 6269-6271, 1987.

[30] J. Ryckaert, G. Ciccotti, H.J.C. Berendsen, “Numerical integration of the cartesian equations of motion of a system with constraints: molecular dynamics of n-alkanes,” *J. Comput. Phys.* vol. 23, pp. 327-341, 1977.
[31] S.Melchionna, G.B.Ciccotti, L.Holian, “Hoover NPT dynamics for systems varying in shape and size,” *Mol. Phys.* Vol. 8, pp. 533-544, 2006.